Strojniški vestnik - Journal of Mechanical Engineering 57(2011)11, 789-798
DOI:10.5545/sv-jme.2011.109
Paper received: 20.05.2011
Paper accepted: 05.09.2011

CW Fiber Laser for Second Harmonic Generation

Vid Novak[1] – Rok Petkovšek[2,*] – Boštjan Podobnik[1] – Janez Možina[2]
[1] LPKF Laser & Elektronika d.o.o, Slovenia
[2] University of Ljubljana, Faculty of Mechanical Engineering, Slovenia

We report on a reduced-complexity laser-diode-seeded master-oscillator-power-amplifier setup of a continuous wave fiber laser, with a single-stage ytterbium doped photonic crystal fiber amplifier. The laser is capable of generating up to 7.5 W single-transverse-mode, narrow-linewidth, polarized output suitable for second harmonic generation. The approach used possesses a further power scaling potential.

Keywords: Yb fiber amplifier, MOPA, narrow-linewidth, single mode, polarized output, second harmonic generation

0 INTRODUCTION

Laser material processing has become a widespread technology in industrial manufacturing [1] to [3]. In various applications, such as e.g. in micro-processing, a high-quality (i.e. single-transverse-mode) output at high power levels is desired [4] to [7]. In conventional laser sources, such as e.g. in bulk solid state lasers, thermally induced optical mode distortions restrict their power scaling potential when a good beam quality needs to be maintained. Therefore, several geometries of the gain medium have been introduced (thin-disc, slab, fiber) in order to overcome these issues.

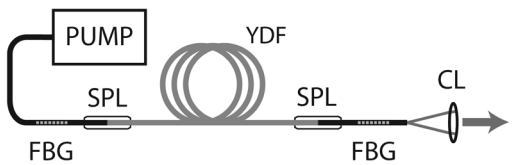

Fig. 1. *Basic fiber laser setup; PUMP: pump source, FBG: fiber Bragg grating, SPL: passive/ active fiber splice, YDF: ytterbium doped fiber, CL: collimator lens*

The fiber laser architecture (Fig. 1) turns out to be a particularly attractive alternative, not only for its capacity to generate raw optical power – up to 10 kW in a single transverse mode has been achieved [8] – but also for a number of other features that distinguish it from other laser setups, and that lead to a rapid penetration of fiber laser systems into applications formerly dominated by other lasers.

An active optical fiber has a rare-earth-doped silica core that serves as a gain medium as well as an optical waveguide that supports only a single transverse mode of propagation, providing long interaction lengths between the gain medium and the guided laser and pump light. A high single-pass-gain gives a low laser threshold and simple amplifier setups are possible even with quasi-three-level dopants such as ytterbium, which offers a high optical-to-optical efficiency [9] due to its low quantum defect.

A low quantum defect, a large surface-to-volume ratio of the core as well as a high damage threshold and low loss of the silica host enable an efficient thermal management and a high-power output. Ytterbium also offers a broad gain bandwidth (975 to 1180 nm) as well as a broad absorption band, covering wavelengths (900 to 980 nm) at which high power semiconductor pump diodes are at their best.

Fully integrated structure provides compact, robust, alignment-free laser setup that is compatible with highly efficient fiber-pigtailed high power pump diodes and various fiber-integrated devices such as e.g. fiber Bragg gratings, fiber couplers, etc.

Fiber lasers also offer the possibility of operating in the pulsed regime. Several different techniques have been employed to achieve a broad pulse parameter space. Active Q-switching in free space coupled [10] to [14] and all-fiber design [14] and [15], passive Q-switching [16] and [17], as well as direct [18] to [20] and external modulation [21] and [22] of a seed laser can be used to generate ns and sub-ns pulse durations

*Corr. Author's Address: University of Ljubljana, Faculty of Mechanical Engineering, Aškerčeva 6, 1000 Ljubljana, Slovenia, rok.petkovsek@fs.uni-lj.si

with PRF (pulse repetition frequency) in the kHz region. In the ps region, semiconductor seed diode gain switching [15] and active modelocking setups [16] can provide pulses with PRF up to the GHz range. Passive modelocking techniques [17] and [18] offer sub 100 fs pulse lengths at PRF of several 100 MHz.

In either pulsed or CW regime, laser (resonator) configurations (Fig. 1) [8] and [27] as well as master oscillator power amplifier (MOPA) configurations (Fig. 2) [7], [28] and [29] can be used for power scaling of fiber lasers. Whereas the laser configuration offers simplicity and compactness, the MOPA approach allows for a more refined control of both temporal and spectral characteristics at high powers. In a MOPA architecture, the output from a highly controlled, low power seed laser can be amplified to high power levels while preserving the desired seed characteristics. Narrow-linewidth operation in CW [19] or pulsed [20] regime and highly-controlled pulsed operation [21] to [24] at high power levels are typically realized using a MOPA design.

A narrow-linewidth output of a MOPA laser can be coherently combined into a synthetic aperture laser with a power scaling potential that can far exceed that of a single-fiber laser. A linearly polarized narrow-linewidth beam can also be efficiently transformed into a higher-order harmonic radiation, e.g. by using a critical phase matching technique in a nonlinear optical crystal. Second harmonic generation (SHG) produces a radiation in the green part of the visible spectrum which can be employed in various industrial and medical applications, such as e.g. thin-film-transistor (TFT) annealing [25], post deposition annealing of ferro-electric thin film for ferro-electric random access memory (FeRAM) and piezoelectric devices [26] or photochemical tooth bleaching [27], where it can significantly outperform existing solutions.

A significant progress has been made in the field of research on narrow-linewidth fiber lasers with reported powers of up to 500 W [19]. MOPA is a well established approach in the field of generating a narrow-linewidth polarized output [19] and [20], that is suitable for SHG. Various seed sources have been used - solid state bulk and fiber laser as well as semiconductor laser diode.

However, multiple-stage amplifiers have had to be used to achieve even a medium power level output (~10W), with each stage requiring a separate pump and thermal management system and a high-power inter-stage optical isolator, rendering such an approach to be rather complex.

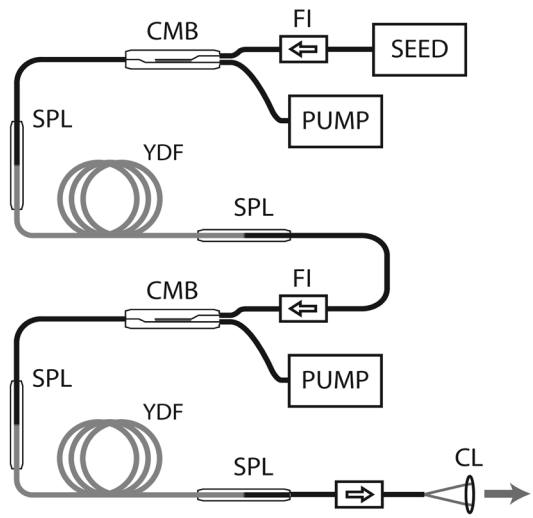

Fig. 2. *MOPA (Master oscillator power amplifier) fiber laser architecture with a two stage fiber amplifier; FI: Faraday isolator, CMB: fiber combiner, SPL: passive/active fiber splice, PUMP: pump source, SEED: seed source, YDF: ytterbium doped fiber, CL: collimator lens*

Recent advances in semiconductor laser diode technology [28] and [29] and the introduction of advanced photonic crystal fiber (PCF) design with an increased pump absorption have opened up a possibility to reduce the complexity of the MOPA architecture.

For the purpose of achieving a single frequency output in the 10 W region, we have focused our work on a diode-seeded single stage amplifier MOPA configuration using an air-clad PCF with ytterbium-doped silica core. Since high gain as well as high efficiency cannot be achieved in a single stage amplifier at the same time, the design had to be optimized to achieve a high enough gain to amplify the seed to the required output power without the need to use excessive pump powers. A single semiconductor single-emitter-based pump module has been proved to be sufficient.

In this paper, a single stage amplifier MOPA arrangement, providing up to 7.5 W of linearly polarized narrow-linewidth output at 1064 nm, suitable for SHG is presented. This simplified arrangement is well-suited for integration into various industrial applications.

1 EXPERIMENTAL SETUP

The experimental setup of our MOPA system is shown in Fig. 3. A 1064 nm continuous wave (CW) fiber-pigtailed semiconductor laser diode master oscillator has been used as a seed source for a single stage ytterbium doped fiber amplifier.

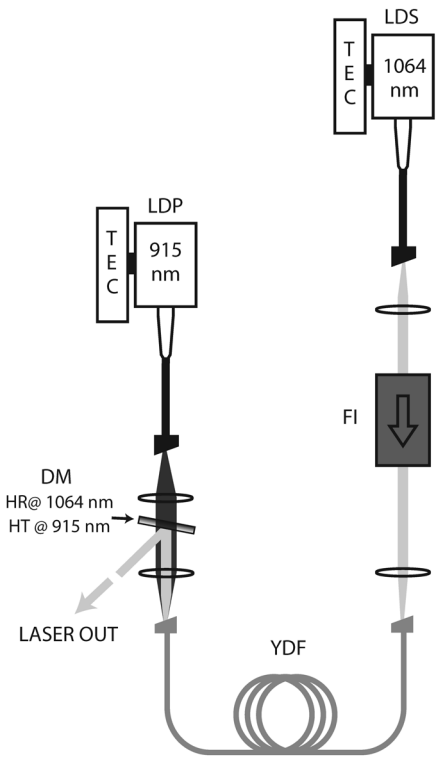

Fig. 3. *Experimental setup of a MOPA system with a semiconductor laser diode master oscillator (i.e. the seed source) and a single stage photonic crystal fiber amplifier; LDS: seed laser diode, LDP: pump laser diode, TEC: thermo-electric cooler, FI: Faraday isolator, DM: dichroic mirror, YDF: ytterbium doped fiber*

The seed diode delivers a narrow-linewidth (300 MHz), single-transverse-mode, linearly polarized beam with an electronically adjustable output power of up to 150 mW. It has been temperature stabilized at 25 °C using a diode-integrated thermo-electric cooler.

An ytterbium-doped photonic-crystal fiber has been used as the amplifier medium. Active fiber's cross section is shown in Fig. 4. Strictly single-transverse mode guidance is achieved, using a step index profile between the 15 μm core with a numerical aperture (*NA*) of 0.055 and the 135 μm inner (pump) cladding (*NA* = 0.6). A microstructured region of air channels, inserted into a silica substrate, that run along the entire fiber length, separates the inner and outer cladding, providing a high-*NA* waveguide for low-brightness pump light. An all-glass pure silica cladding structure (i.e. the absence of a polymer outer cladding) alleviates the risk of fiber damage at high levels of launched pump power and offers a significant power scaling potential.

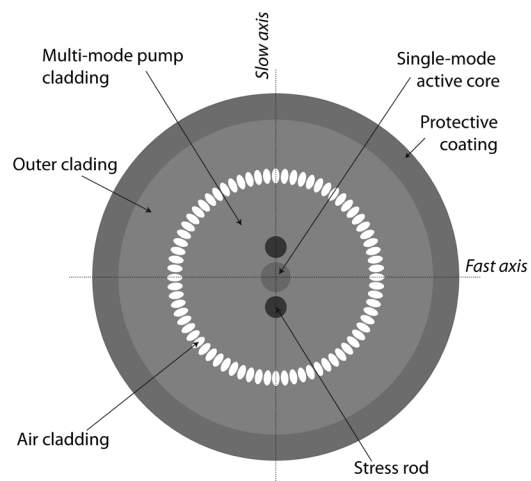

Fig. 4. *Active fiber cross section. Strictly single-transverse-mode guiding is achieved, using a step index profile between the core and the inner cladding; polarization maintaining fiber has two orthogonal axes of propagation, a slow and a fast one, which are generated by the stress rods on each side of the core; air cladding region separates the inner and the outer cladding, providing a high NA waveguide for low-brightness pump light*

The active fiber is polarization maintained (PM) with two orthogonal axes of propagation. A strong birefringence is created by inducing a

constant stress-field within the fiber core by using stress-applying members on each side of the core. Birefringence breaks the circular symmetry, thus creating two principal transmission axes within the core, providing a strong isolation against cross-coupling of guided light between the two orthogonal eigenmodes, while the fiber is being subjected to external stress and temperature perturbations along its length.

PM fiber's birefringence axis has been aligned with the seed polarization plane in order to excite a single polarization mode and thus maintain the polarization state along the amplification path in the PM fiber.

A fiber pigtailed 915 nm semiconductor laser diode delivering up to 25 W in the CW regime has been used as the pump source for the fiber amplifier in a counter-propagating pumping scheme. An electronically controllable current source has been used as the pump diode driver while an external thermo-electric cooler provides the means for a temperature-stabilized diode operation at peak absorption wavelength.

Both the seed and the pump beam have been free-space coupled into the fiber amplifier using bulk optics. The coupling efficiency has been determined, using a short fiber piece, to be 75 and 80% for the seed and pump beam respectively. The absorption of the 915 nm pump light in the core has also been measured, obtaining a value of 90%.

The fiber ends have been precisely cleaved at an angle of approximately 8° to the fiber axis to prevent parasitic lasing in the amplifier due to the Fresnel back-reflection on the fiber facets, effectively coupling the back-reflected light into radiation modes and thus preventing their amplification in the backward direction.

A dichroic mirror has been used to separate the amplified laser beam and the input pump beam on the output side of the amplifier.

The high amplifier gain necessitates the use of an optical isolator to protect the seed source against the amplified back-reflected beam. A bulk optic Faraday isolator with 42 dB isolation has therefore been inserted between the seed source and the fiber amplifier input.

2 EXPERIMENTAL RESULTS AND DISCUSSION

Experimental results have been grouped into the following subsections: Output power and amplifier gain, Amplifier efficiency, Polarization contrast, Output power stability and Emission spectrum.

2.1 Output Power and Amplifier Gain

Electronically adjustable seed current that drives the semiconductor master oscillator allows for a refined control over the optical seed power coupled into the fiber amplifier. Data were acquired by varying the seed current and by simultaneously recording the resulting output power. Fig. 5 shows the 1064 nm laser output power P_L from the ytterbium PCF amplifier as a function of the input seed power P_s at several different levels of launched pump power P_p.

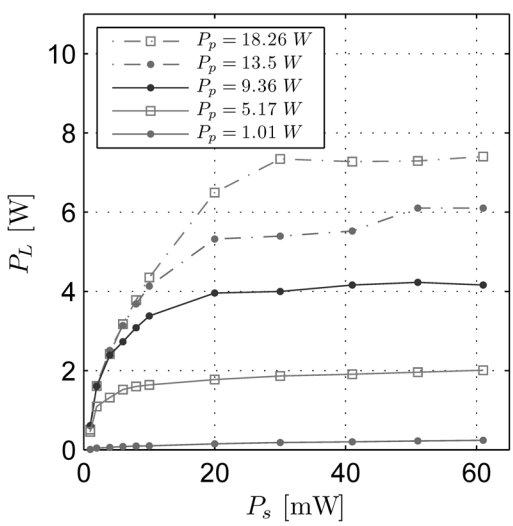

Fig. 5. *Average laser output power P_L versus launched seed power P_s; the legend shows the pump power P_p used, for each graph respectively*

With increasing seed power the gain saturates and the output power only becomes a function of the launched pump power in the saturated regime. The output power scales linearly with pump power up to approx. 15 W of pump power, whereas a transition into a sub-linear

relationship is observed above this value due to pump saturation.

A maximum output power of 7.5 W at 1064 nm was achieved in the saturated regime for a launched pump power of 18.3 W, corresponding to a single pass gain of approximately 24 dB. The maximum achievable output power was only limited by the available pump power.

Fig. 6 shows the amplifier gain characteristics. Amplifier gain P_L / P_s as a function of launched seed power P_s has been plotted for various levels of pump power P_p.

The gain increases monotonically with pump power and decreases monotonically with seed power. A maximum gain of 29.5 dB has been achieved at the seed power of 2 mW and pump power of 18.3 W.

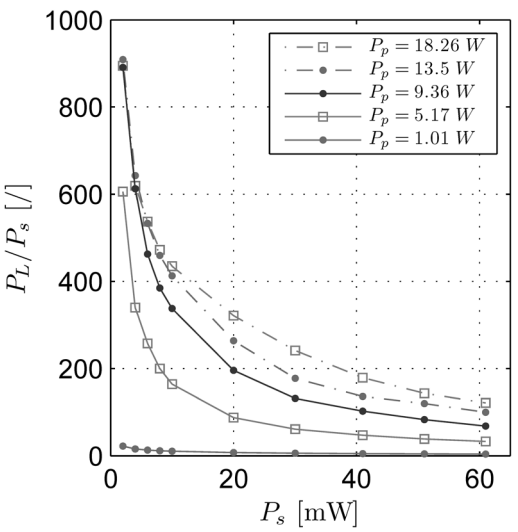

Fig. 6. *Amplifier gain P_L / P_s as a function of launched seed power P_s; the legend shows the pump power P_p used, for each individual graph*

Notice that by reducing the seed power the small signal gain becomes increasingly saturated with respect to launched pump power.

2.2 Amplifier Efficiency

A single-stage single-pass amplifier inherently suffers from a lower optical-to-optical efficiency than a multiple stage amplifier where the overall efficiency is predominantly determined by the highly efficient final power amplifier stage that operates in the highly saturated regime throughout the whole fiber length.

Here, a single-stage single-pass amplifier has been used in order to reduce the complexity of the laser setup, rendering the high levels of efficiency out of reach since the input segment of the amplifier cannot be saturated and acts therefore, as an amplified stimulated emission (ASE) source.

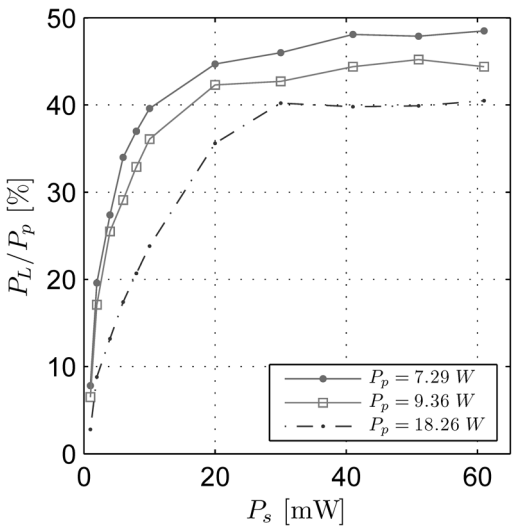

Fig. 7. *Fiber amplifier efficiency P_L / P_p versus the seed power P_s for three different levels of pump power P_p (as shown in the legend); efficiency is defined here as a quotient of total output power at 1064 nm P_L versus the pump power launched into the active fiber P_p*

Therefore, a careful amplifier design optimization has been undertaken in order to achieve a high enough gain to amplify the seed to the required output power, as well as to get a reduced ASE output and the highest possible efficiency, so that only one single-emitter based pumping module would be sufficient to pump the amplifier, leading to a simpler thermal management and pump driver system.

An air-clad PCF with a strong overlap between the pump modes and the active core that is a direct consequence of a high-*NA* (0.6), small diameter (135 μm) pump cladding has been used to ensure a high pump light absorption, leading to a short unsaturated length of the amplifier,

effectively reducing the ASE output. A plot of amplifier efficiency P_L / P_p as a function of the launched seed power P_s is shown in Fig. 7. Efficiencies up to 50% have been achieved as well as a laser-to-ASE contrast up to 10 dB as shown in Fig. 8.

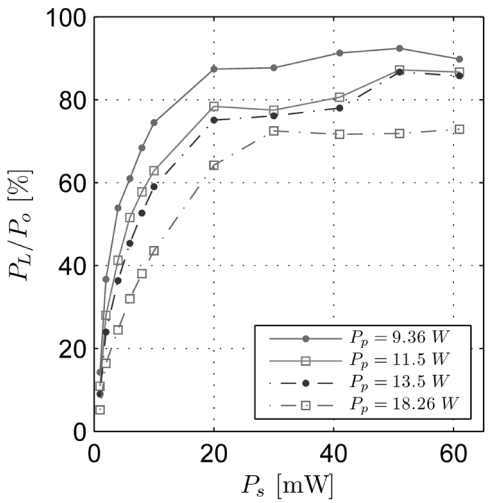

Fig. 8. *Percentage of laser power P_L (i.e. power at 1064 nm) in the amplifier output P_o as a function of launched seed power P_s; the legend shows the pump power P_p used, for each graph respectively*

2.3 Polarization Contrast

The 1064 nm output of the amplifier is linearly polarized. Fig. 9 shows the dependence of the polarization contrast on the launched pump power P_p at 10 mW of input seed power P_s. The polarization contrast has been measured using a rotating beam-splitter cube and is defined here as a ratio of maximum vs. minimum transmitted power P_{max} / P_{min} at 1064 nm.

Whereas a high contrast of approx. 100 to 120 could be maintained up to approx. 10 W of pump power, a reduction of the achievable contrast is observed when approaching higher levels. Nevertheless, a value of over 30 could be achieved over the entire range.

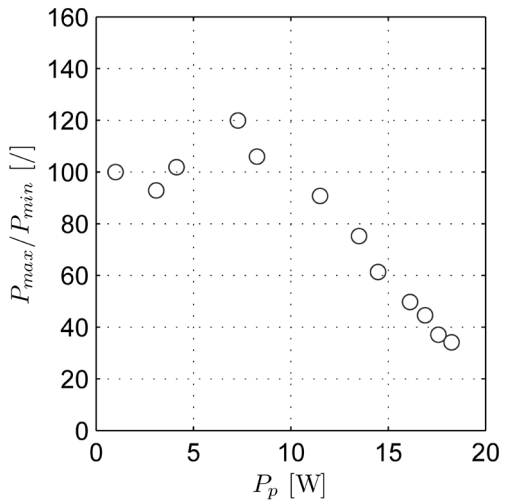

Fig. 9. *Output beam polarization contrast P_{max} / P_{min} at 1064 nm versus the launched pump power P_p at 10 mW of seed power P_s*

2.4 Output Power Stability

A long term (1 hour) as well as short term (2 s) output power stability has been measured using a thermopile sensor and a photodiode respectively.

The output power stability on the 1 h scale was measured to be 1.3% RMS and 2.4% on the 2 s scale.

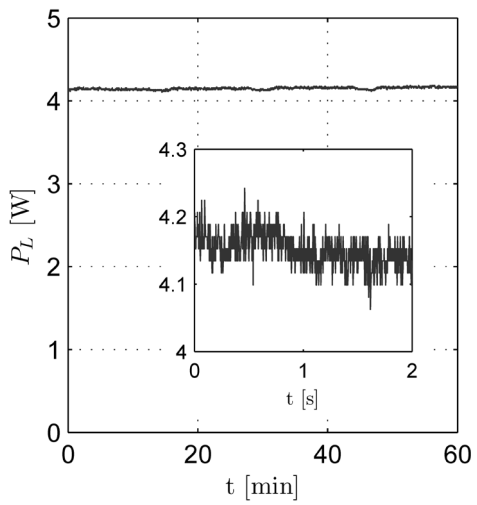

Fig. 10. *Output power (P_L) stability over an interval of 1 hour, measured using a thermopile sensor; photodiode measured short term stability on the seconds scale is shown on the inset*

2.5 Emission Spectrum

The emission spectrum of the amplifier output has been investigated using an optical spectrum analyzer (OSA). In addition to the 1064 nm signal, the spectrum also exhibits an ASE band, as shown in Figs. 11 and 12.

The overall amplifier spectral fidelity could not be determined using an OSA due to its limited resolution bandwidth (70 pm) that is orders of magnitude wider than that required to sample a 300 MHz laser line at 1064 nm. However, it still enabled us to examine various ASE spectral features that were present in the amplifier output.

A 5-by-2 matrix of optical spectra is given in Fig. 11, providing a comparison of the unsaturated versus the saturated operation of the amplifier at various pump and seed powers used. A row-vise comparison shows that at low pump powers, no significant ASE is present. However, a significant build-up of ASE can be observed when the pump is increased. An even further increase results in the onset of spurious lasing as confirmed by the presence of sharp peaks in the

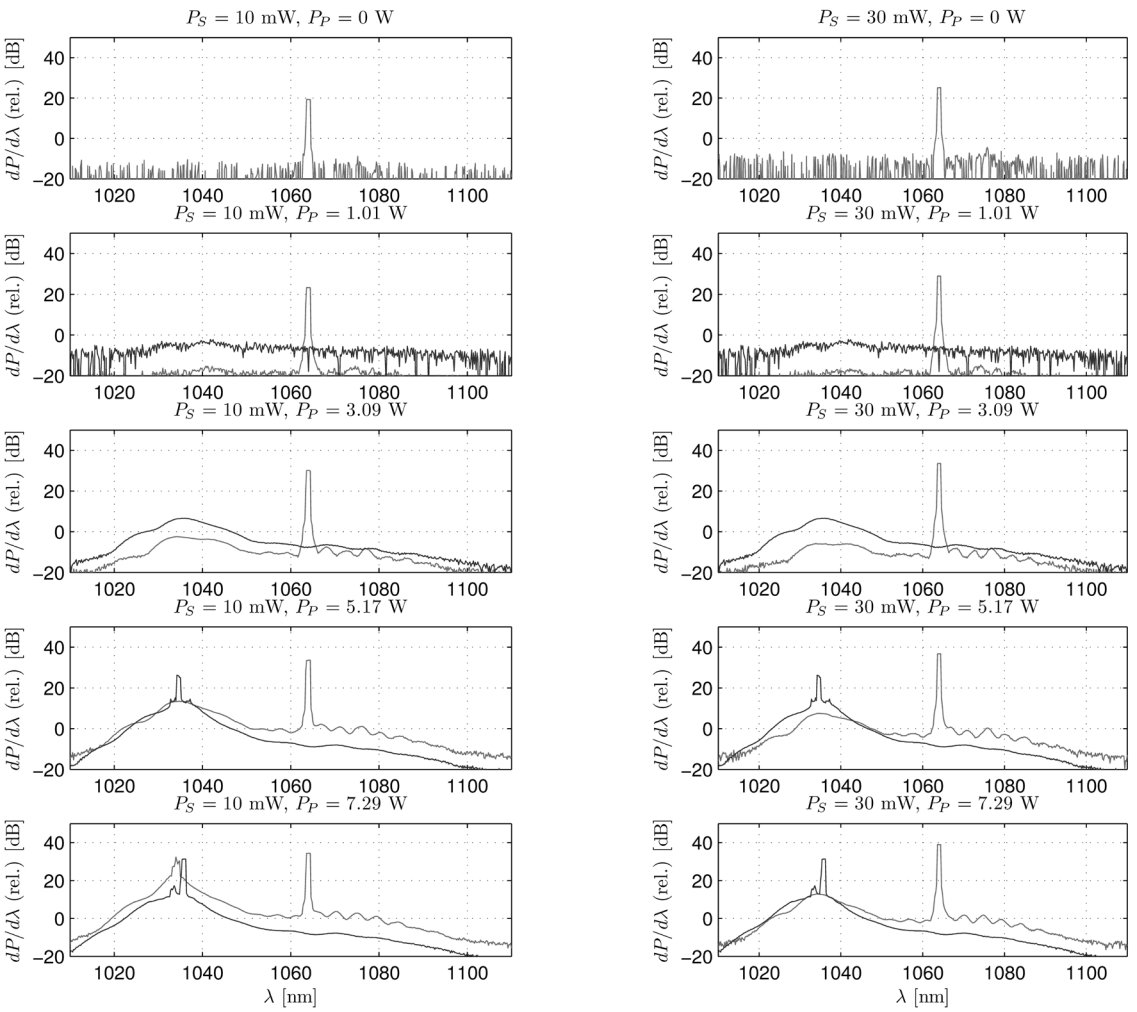

Fig. 11. *Output power spectrum comparison between the unsaturated and saturated regime; a 5-by-2 matrix of optical spectra is given, where the bright line in the left and right columns represents the spectrum at launched seed powers P_s of 10 and 30 mW respectively, whereas the first, second, third, fourth and fifth row refer to launched pump powers P_p of 0, 1.01, 3.09, 5.17 and 7.29 W respectively; unseeded amplifier response is given as a comparison for rows 2 to 5 (dark line)*

ASE spectrum. Introducing a 10 mW seed signal into the amplifier causes a significant reduction of ASE only at lower pump powers but it does not suppress the lasing modes at higher pumping levels.

A column-wise comparison on the other hand shows that by increasing the seed power the gain can be saturated and consequently, the ASE modes effectively suppressed even at the highest pumping levels. The seed diode optical output has been sufficient to maintain a spurious-lasing free operation throughout the entire range of pump powers. Fig. 12 shows the output power spectrum in the highly saturated regime at a seed power of 57 mW and at four different pump levels.

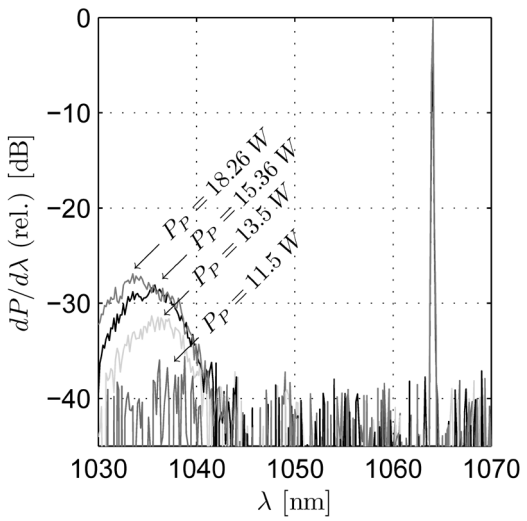

Fig. 12. *Output power spectrum in the highly saturated regime at a seed power P_s of 57 mW and at four different levels of launched pump power P_P (as shown on the graph); a rise of approx. 10 dB of ASE spectrum peak is observed, as well as a slight shift of the ASE peak towards lower wavelengths*

The ASE spectral features lie more than 26 dB below the signal level without any evidence of the lasing modes being present.

3 CONCLUSION

We have demonstrated a reduced complexity MOPA system with a single-stage ytterbium PCF amplifier, generating up to 7.5 W single-transverse-mode linearly-polarized narrow-linewidth output suitable for second harmonic generation. Amplifier gain of 24 dB at the highest optical output power has been achieved and we have managed to maintain the polarization contrast of over 30 throughout the entire output power range. Amplifier efficiencies up to 50% and laser-to-ASE contrasts of up to 10 dB have been obtained.

The presented setup has the potential to be fully fiber integrated and scaled well above the 10 W level since its output has only been limited by the currently available pump power.

4 ACKNOWLEDGMENT

The operation has been partly financed by the European Union, European Social Fund.

5 REFERENCES

[1] Steen, W.M. (2003). Laser material processing – an overview. *Journal of Optics A: Pure and Applied Optics,* vol. 5, no. 4, p. S3-S7.

[2] Steiger, E. (2007). What is the best choice for laser material processing – rod, disk, slab or fiber. *26th international congress on applications of lasers and electro-optics Conference Proceedings*.

[3] Kek, T., Grum, J. (2010). Influence of the graphite absorber during laser surface hardening. *Strojniški vestnik - Journal of Mechanical Engineering,* vol. 56, no. 2, p. 150-157.

[4] Hoult, T., Gabzdyl, J. (2008). Fiberlaser: beam sources and applications. *Laser Technik Journal,* vol. 5, no. 3, p. 37-40.

[5] Gabzdyl, J. (2010). Micro-machining with nanosecond pulsed fiber laser beams. *PICALO Pacific International Conference on Applications of Lasers & Optics Conference Proceedings*, p. M606.

[6] Gabzdyl, J. (2010). Micro-cutting with nanosecond pulsed fiber lasers. *ICALEO, 29th International Congress on Applications of Lasers & Electro-Optics Conference Proceedings*, p. M901.

[7] Hoult, T., Gabzdyl, J., Dzurko, K. (2008). Fiber lasers in solar applications. *Solar Energy: New Materials and Nanostructured*

Devices for High Efficiency Conference Proceedings, p. STuC3.

[8] Stiles, E. (2009). New developments in IPG fiber laser technology. *5th International Workshop on Fiber Lasers Conference Proceedings*.

[9] Jeong, Y.C., Boyland, A.J., Sahu, J.K., Chung, S.H., Nilsson, J., Payne, D.N. (2009). Multi-kilowatt single-mode ytterbium-doped large-core fiber laser. *Journal of the Optical Society of Korea,* vol. 13, no. 4, p. 416-422.

[10] Limpert, J., Höfer, S., Liem, A., Zellmer, H., Tünnermann, A., Knoke, S., Voelckel, H. (2002). 100-W average-power, high-energy nanosecond fiber amplifier. *Applied Physics B: Lasers and Optics,* vol. 75, no. 4, p. 477-479.

[11] Limpert, J., Deguil-Robin, N., Petit, S., Manek-Hönninger, I., Salin, F., Rigail, P., Hönninger, C., Mottay, E. (2005). High power Q-switched Yb-doped photonic crystal fiber laser producing sub-10 ns pulses. *Applied Physics B: Lasers and Optics,* vol. 81, no. 1, p. 19-21.

[12] Schmidt, O., Rothhardt, J., Röser, F., Linke, S., Schreiber, T., Rademaker, K., Limpert, J., Ermeneux, S., Yvernault, P., Salin, F. (2007). Millijoule pulse energy Q-switched short-length fiber laser. *Optics Letters,* vol. 32, no. 11, p. 1551-1553.

[13] Bammer, F., Petkovšek, R. (2007). Q-switching of a fiber laser with a single crystal photo-elastic modulator. *Optics Express,* vol. 15, no. 10, p. 6177-6182.

[14] Petkovšek, R., Bammer, F., Schuoecker, D., Možina, J. (2009). Dual-mode single-crystal photoelastic modulator and possible applications. *Applied Optics,* vol. 48, no. 7, p. C86-C91.

[15] Dupriez, P., Piper, A., Malinowski, A., Sahu, J.K., Ibsen, M., Thomsen, B.C., Jeong, Y., Hickey, L.M.B., Zervas, M.N., Nilsson, J., Richardson, D.J. (2006). High average power, high repetition rate, picosecond pulsed fiber master oscillator power amplifier source seeded by a gain-switched laser diode at 1060 nm. *IEEE Photonics Technology Letters,* vol. 18, no. 9, p. 1013-1015.

[16] Adhimoolam, B., Hekelaar, M.G., Gross, P., Lindsay, I.D., Boller, K.J. (2006). Wavelength-tunable short-pulse diode-laser fiber-amplifier system around 1.06 um. *IEEE Photonics Technology Letters,* vol. 18, no. 7, p. 838-840.

[17] Röser, F., Schimpf, D., Schmidt, O., Ortaç, B., Rademaker, K., Limpert, J., Tünnermann, A. (2007). 90 W average power 100 uJ energy femtosecond fiber chirped-pulse amplification system. *Optics Letters,* vol. 32, no. 15, p. 2230-2232.

[18] Ortaç, B., Baumgartl, M., Limpert, J., Tünnermann, A. (2009). Approaching microjoule-level pulse energy with mode-locked femtosecond fiber lasers. *Optics Letters,* vol. 34, no. 10, p. 1585-1587.

[19] Jeong, Y., Nilsson, J., Sahu, J.K., Payne, D.N., Horley, R., Hickey, L.M.B., Turner, P.W. (2007). Power scaling of single-frequency ytterbium-doped fiber master-oscillator power-amplifier sources up to 500 W. *IEEE Journal of Selected Topics in Quantum Electronics,* vol. 13, no. 3, p. 546-551.

[20] Babushkin, A.V., Gapontsev, D.V., Platonov, N.S., Gapontsev, V.P. (2006). Pulsed fiber laser with 30 W output power at 532 nm. *Fiber Lasers III: Technology, Systems, and Applications SPIE Conference Proceedings*, vol. 6102, p. 334-338.

[21] Vu, K.T., Malinowski, A., Richardson, D.J., Ghiringhelli, F., Hickey, L.M.B., Zervas, M.N. (2006). Adaptive pulse shape control in a diode-seeded nanosecond fiber MOPA system. *Optics Express,* vol. 14, no. 23, p. 10996-11001.

[22] Schimpf, D.N., Limpert, J., Tunnermann, A., Salin, F. (2008). Seed pulse optimization for saturated fiber-amplifiers. *Conference on Lasers and Electro-Optics/Quantum Electronics and Laser Science Conference Proceedings*, p. 1-2.

[23] Malinowski, A., Vu, K.T., Chen, K.K., Nilsson, J., Jeong, Y., Alam, S., Lin, D., Richardson, D.J. (2009). High power pulsed fiber MOPA system incorporating electro-optic modulator based adaptive pulse shaping. *Optics Express,* vol. 17, no. 23, p. 20927-20937.

[24] Lin, D., Alam, S.-U., Chen, K., Malinowski, A., Norman, S., Richardson, D. (2009). 100 W, fully-fiberised ytterbium doped master oscillator power amplifier incorporating adaptive pulse shaping. *Lasers and Electro-Optics / International Quantum Electronics Conference Proceedings*, p. CFM4.

[25] Sugawara, Y., Uraoka, Y., Yano, H., Hatayama, T., Fuyuki, T., Mimura, A. (2007). Crystallization of double-layered silicon thin films by solid green laser annealing for high-performance thin-film transistors. *IEEE Electron Device Letters,* vol. 28, no. 5, p. 395-397.

[26] Jiang, J., Kuroki, S.I., Kotani, K., Ito, T. (2010). Ferroelectric properties of lead zirconate titanate thin film on glass substrate crystallized by continuous-wave green laser annealing. *Japanese Journal of Applied Physics,* vol. 49, no. 4.

[27] Goharkhay, K., Schoop, U., Wernisch, J., Hartl, S., De Moor, R., Moritz, A. (2009). Frequency doubled neodymium: yttrium-aluminum-garnet and diode laser-activated power bleaching-pH, environmental scanning electron microscopy, and colorimetric in vitro evaluations. *Lasers in Medical Science,* vol. 24, no. 3, p. 339-346.

[28] Osowski, M.L., Hu, W., Lammert, R.M., Liu, T., Ma, Y., Oh, S.W., Panja, C., Rudy, P.T., Stakelon, T., Ungar, J.E. (2007). High brightness semiconductor lasers. *SPIE Photonics West Conference Proceedings*, vol. 6456, p. 64560D-1.

[29] Lammert, R.M., Oh, S.W., Osowski, M.L., Panja, C., Rudy, P.T., Stakelon, T.S., Ungar, J.E. (2006). Advances in high brightness semiconductor lasers. *SPIE Conference Proceedings*, vol. 6104, p. 61040I.